THE JOURNAL OF PHYSICAL CHEMISTRY A

Article

pubs.acs.org/JPCA

Circular Dichroism Spectra of Uridine Derivatives: ChiraSac Study

Tomoo Miyahara,[†] Hiroshi Nakatsuji,*[,†,‡] and Takehiko Wada[‡]

[†]Quantum Chemistry Research Institute (QCRI), JST-CREST, Kyodai Katsura Venture Plaza, North Building 107, 1-36 Goryo-Oohara, Nishikyo-ku, Kyoto, 615-8245, Japan

[‡]Institute of Multidisciplinary Research for Advanced Materials, Tohoku University, 2-1-1, Katahira, Aoba-ku, Sendai 980-8577, Japan

Supporting Information

ABSTRACT: The experimental circular dichroism (CD) spectra of uridine and NH2-uridine that were different in the intensity and shape were studied in the light of the ChiraSac method. The theoretical CD spectra at several different conformations using the symmetry-adapted-cluster configuration-interaction (SAC-CI) theory largely depended on the conformational angle, but those of the anti-conformers and the Boltzmann average reproduced the experimentally obtained CD spectra of both uridine and NH2-uridine. The differences in the CD spectra between the two uridine derivatives were analyzed by using the angle θ between the electric transition dipole moment (ETDM) and the magnetic transition dipole moment (MTDM).

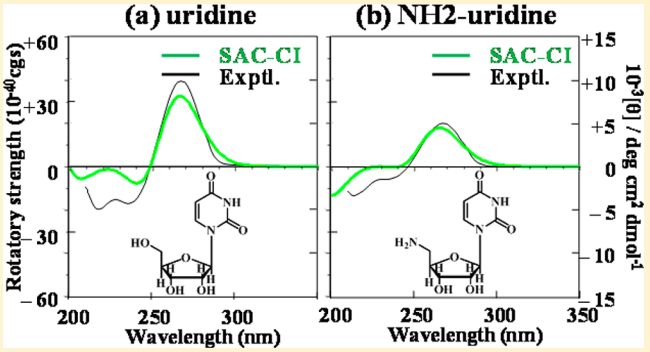

1. INTRODUCTION

Circular dichroism (CD) spectroscopy combined with the reliable theoretical analysis is a powerful technique for conformational analysis.[1,2] The CD spectra can distinguish between the right- and left-handed helical structures of DNA. In addition, the CD spectra can also determine the conformation of nucleic acid bases. A reliable theoretical method is necessary to analyze the conformational dependences of the CD spectra, and the symmetry-adapted-cluster configuration-interaction (SAC-CI) theory[3−8] was shown to provide reliable CD spectra.[2,9,10] Previously, we reported that the dihedral angle between the guanine and the deoxyribose in deoxyguanosine had a drastic effect on the sign and the intensity of the SAC-CI CD spectrum.[10] In addition, it became clear that the SAC-CI CD spectra are very sensitive to the rotation around single bond near the chiral atoms in α-hydroxyphenylacetic acid.[2] These imply that the reliable excited-state theory can be a useful tool for elucidating the chemistry driven by the low-energy processes involving chiral molecules. Several research groups have also demonstrated that the CD spectra of chiral molecules are sensitive to the conformational changes of the molecules.[11−23] In such studies, we need a highly reliable theory because a poorly reliable theory may lead to an erroneous result. Recently, the time-dependent density functional theory (Td-DFT) using the PBE0 functional and the SAC-CI calculations showed reasonable agreement in both transition energies and excited-state equilibrium structures.[24,25] Although the SAC-CI method is more expensive than the Td-DFT method, the SAC-CI method provides more reliable predictions of spectroscopic properties. Reliable ground-state geometry, which is also necessary to obtain the SAC-CI CD spectra, can be calculated using the Hartree−Fock (HF) and DFT[26] at lower cost than using the SAC method. The polarizable continuum model (PCM)[27] and AMBER[28] may also be used to represent the effects of the surrounding molecules such as the solvent and the protein. The Gaussian suite of programs[29] and its newer 09 version now available include all of these programs.

Recently, we have undertaken a new molecular technology, "ChiraSac", which analyzes the chiral molecular systems using the SAC-CI method on Gausssain. The overview of a ChiraSac project is shown in Figure 1. The term ChiraSac is derived from "Chira" of chirality and "Sac" of SAC-CI, respectively. We have displayed the concept of ChiraSac in some details in a recent paper.[2] We can use not only the SAC-CI methodology but also many other useful methods included in the Gaussian suite of programs. The ChiraSac clarifies the relationship between the structure of a chiral molecule and its CD spectrum as well as providing us with chemical information about weak interactions such as hydrogen-bonding and stacking in DNA.[10] In this way, the ChiraSac can reveal the weak interactions behind the observed CD spectra. The ChiraSac also provides the chemical and biological information on chiral molecules in solution and in protein environment. This chemical and biological information is valuable for doing molecular design.

Figure 2 shows the experimental CD[30] and UV[31] spectra of uridine and NH2-uridine compared with the SAC-CI CD and UV Boltzmann average spectra. Uridine is a component molecule of RNA and is composed of uracil, a nucleic acid base, and ribose. NH2-Uridine contains an amino (NH_2) substituent at the C5′ position of ribose instead of the hydroxyl (OH) group as seen

Received: February 24, 2014
Revised: March 26, 2014
Published: March 28, 2014

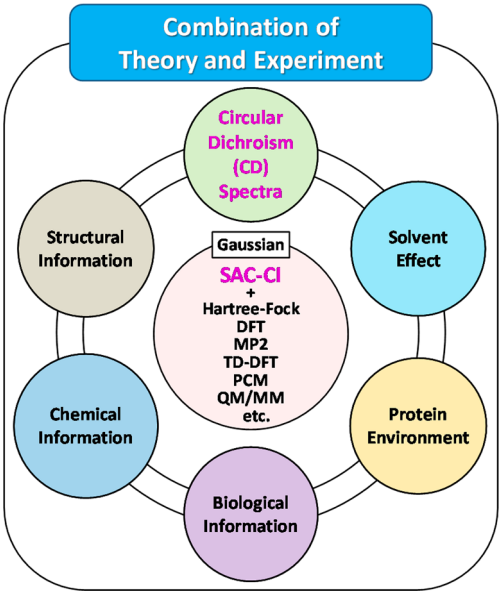

Figure 1. Overview diagram of a ChiraSac project.

from Figure 2a,c. There are four chiral carbons in the ribose of both uridine and NH2-uridine (see Figure S1, Supporting Information). The experimental CD spectrum of NH2-uridine differs from that of uridine,[30] displaying a weaker intensity than that for uridine, although the excited states of two molecules have almost the same configurations localized around the uracil (Figures 2a,c). We varied the dihedral angle between uracil and ribose a few at a time in both uridine and NH2-uridine and calculated the CD spectra using the SAC-CI theory.[3−8] The Boltzmann-averaged SAC-CI CD spectra, which were obtained from these calculations, reproduced well the features of the experimental CD spectra, though we did not examine the effects of the solvents in this article. This result explained the origin of the difference in the CD spectra between uridine and NH2-uridine.

2. COMPUTATIONAL DETAILS

The ground-state geometries of uridine and NH2-uridine were optimized using Gaussian09[29] with the Hartree−Fock calculations of D95(d)[32] basis set. For the SAC/SAC-CI calculations, the basis functions employed were D95(d),[32] the core orbitals of the C, O, and N atoms were treated as frozen orbitals, and all single and selected double excitation operators were included. Perturbation selection[33] was carried out with the threshold sets of 5×10^{-7} and 1×10^{-7} hartree for the SAC and SAC-CI calculations, respectively. The SAC-CI UV and CD spectra were

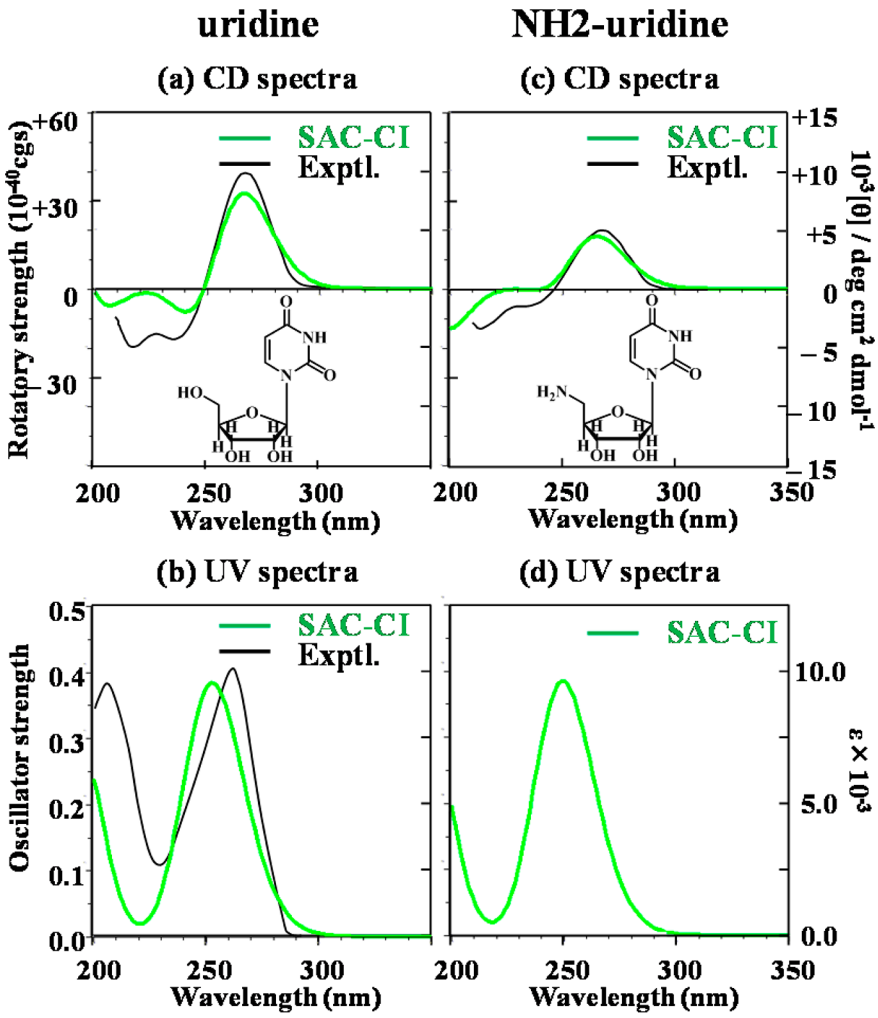

Figure 2. Experimental CD (a,c)[30] and UV (b,d)[31] spectra (black lines) of uridine (a,b) and NH2-uridine (c,d) compared with the SAC-CI CD and UV Boltzmann average spectra (green lines).

dx.doi.org/10.1021/jp501906u | J. Phys. Chem. A 2014, 118, 2931−2941

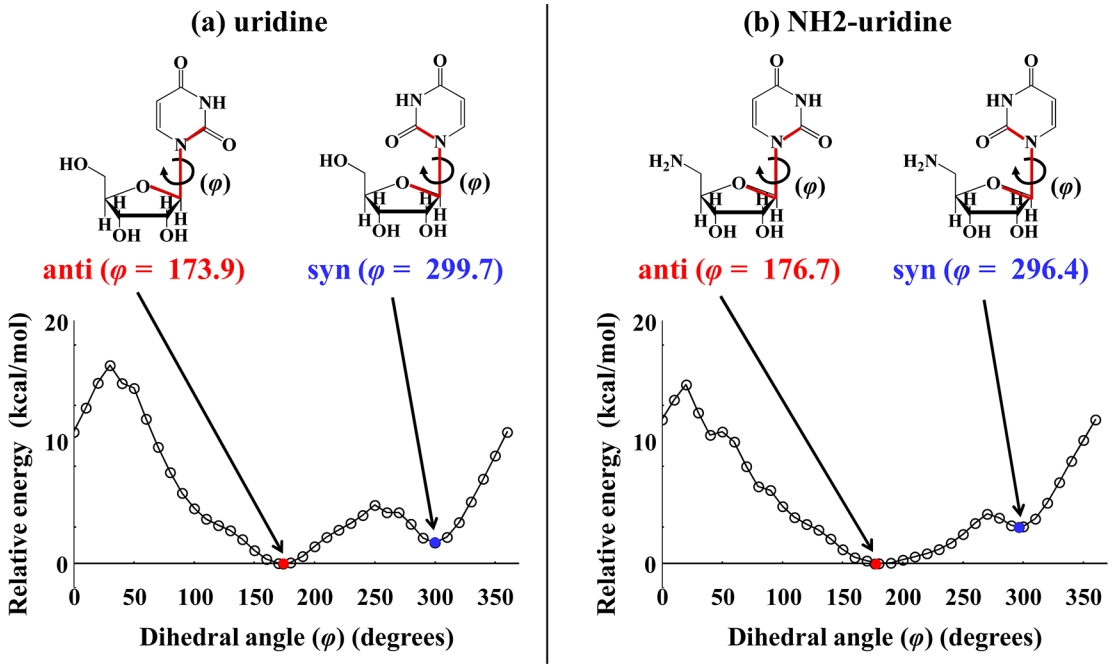

Figure 3. Potential energy curves of the ground state of (a) uridine and (b) NH2-uridine.

convoluted using Gaussian envelopes to describe the Franck–Condon widths and the resolution of the spectrometer. The full width at half-maximum (fwhm) of the Gaussian envelope was 0.6 eV. The rotatory strengths (R_{0a}) of the CD spectra were calculated using the gauge-invariant velocity form given by the following equation:

$$R_{0a} = \mathrm{Im}\left\{\frac{\langle\Psi_0|\nabla|\Psi_a\rangle\langle\Psi_a|\hat{m}|\Psi_0\rangle}{E_a - E_0}\right\} \quad (1)$$

where Ψ_0 and Ψ_a are the ground and excited states, respectively, and $\hat{m}$ is the magnetic dipole moment operator.

Below, we showed the results of the SAC-CI calculations, which are really ab initio: we did not do any frequency and intensity scaling, not like in the Td-DFT calculations.

3. GROUND STATE GEOMETRIES

We explain the relationship between the ground-state stability and the dihedral angle (φ) between ribose and uracil in this section. We calculated the changes in the potential energy for the ground state of the uridine and NH2-uridine as a function of changes in the dihedral angle (φ) between ribose and uracil as shown in Figure 3a,b. The dihedral angle (φ) was varied by increments of 10° and all of the geometrical parameters except for the dihedral angle were optimized. In the anti-region, the fully optimized dihedral angle was calculated to be 173.9° for uridine and 176.7° for NH2-uridine. However, the optimized dihedral angle of the syn-region was calculated to be 299.7° for uridine and 296.4° for NH2-uridine. The anti-conformation was more stable than the syn-conformation by 1.73 kcal/mol for uridine and by 3.00 kcal/mol for NH2-uridine. The optimized geometries of the anti and syn-conformers of uridine and NH2-uridine are shown in Supporting Information, Table S1 to S4.

The potential energy curves were similar between both uridine derivatives. The anti-conformation is converted easily to the syn-conformation by rotation in the clockwise direction (the direction of the arrow in Figure 3a,b) because the energy barrier was only ~5 kcal/mol. However, the rotation in the counterclockwise direction would be more difficult because the energy barrier was approximately ~15 kcal/mol. Both potential energy curves were flat in the anti-region and sharp in the syn-region because both uridine derivatives have an intramolecular hydrogen-bond in the syn-region. The oxygen atom of the uracil forms a hydrogen bond to the hydroxyl group of C5′ for uridine and to the amino group of C5′ for NH2-uridine. The hydrogen bond distance was 2.93 Å for uridine and 3.21 Å for NH2-uridine, respectively. Since the hydrogen bond of uridine is stronger than that of NH2-uridine, the energy difference between the anti- and syn-conformers is smaller for uridine but larger for NH2-uridine. Therefore, the syn-conformer contributed to the Boltzmann averaged SAC-CI spectrum of uridine more than that of NH2-uridine (see Tables 1 and 2).

Table 1. Existence Ratios of Uridine from the Boltzmann Distributions at 298.15 K

dihedral angle (φ°)	existence ratio (%)	dihedral angle (φ°)	existence ratio (%)	dihedral angle (φ°)	existence ratio (%)
10–100	<0.1	173.9 (anti)	36.2	240–270	<0.1
110	0.1	180	21.7	280	0.1
120	0.2	190	11.2	290	0.8
130	0.3	200	2.9	299.7 (syn)	1.7
140	1.1	210	0.8	310	0.8
150	4.9	220	0.3	320	0.1
160	16.6	230	0.1	330–360	<0.1

However, NH2-uridine had different features from uridine in the following points except for the optimized dihedral angle of the anti-conformer and the energy difference between anti- and syn-conformers, as described above. In the anti-region, the potential energy curve for NH2-uridine was flatter than for uridine, which implied that NH2-uridine can rotate more flexibly than uridine. The anti-conformer can convert to the syn-conformer more easily in NH2-uridine than in uridine because the energy barrier of NH2-uridine is lower than that of uridine.

dx.doi.org/10.1021/jp501906u | J. Phys. Chem. A 2014, 118, 2931–2941

Table 2. Existence Ratios of NH2-Uridine from the Boltzmann Distributions at 298.15 K

dihedral angle (φ°)	existence ratio (%)	dihedral angle (φ°)	existence ratio (%)	dihedral angle (φ°)	existence ratio (%)
10−110	<0.1	176.7 (anti)	24.9	250	0.4
120	0.1	190	16.2	260	0.1
130	0.2	200	12.8	270−280	<0.1
140	0.7	210	8.2	290	0.1
150	3.0	220	5.3	296.4 (syn)	0.2
160	9.2	230	3.0	310−360	<0.1
170	14.4	240	1.2		

4. CD SPECTRA OF URIDINE

In this section, for uridine, we explain the relationship between the CD spectra and the dihedral angle (φ). The SAC-CI CD spectra (red) of uridine at several dihedral angles (Figure 4a−w) and the SAC-CI CD Boltzmann average spectrum (Figure 4x) were compared with the experimentally obtained CD spectrum (black) above 200 nm. In the experimental CD spectrum,[30] the first band was strongly positive at 267 nm (4.64 eV). The second and third bands were weakly negative at 235 nm (5.28 eV) and 217 nm (5.71 eV). The fourth band with a strongly positive peak was observed below 200 nm.[31]

The experimental CD spectrum agreed well with the SAC-CI CD spectrum of the most stable anti-conformation (Figure 4j) and the surroundings with φ = 160 and 180° (Figure 4i,k), but was very different from those of other conformers. When the uridine rotates in a clockwise direction from the anti-conformation, the SAC-CI CD spectra with a broad positive peak changed gradually from φ = 190° to φ = 250°. After passing the top of the potential energy curve at φ = 250°, the peak with a negative sign appeared in the lowest energy region between φ = 290° and φ = 350°. For the syn-conformation, the SAC-CI CD spectrum was completely opposite to the experimental CD spectrum (Figure 4t). The features of the SAC-CI CD spectra are the same between φ = 290° and φ = 350°, although their intensities are different. After crossing the line of the highest peak of the potential energy curve (Figure 3a), the SAC-CI CD spectra drastically changed between φ = 10° and φ = 30° (Figure 4a,b). The SAC-CI CD spectra between φ = 30° and φ = 130° exhibited the opposite features to those observed between φ = 190° and φ = 250°. These results indicate that the CD spectra are strongly dependent on the dihedral angle between uracil and ribose.

5. CD SPECTRA OF NH2-URIDINE

In this section, for NH2-uridine, we explain the relationship between the CD spectra and the dihedral angle (φ). The SAC-CI CD spectra (red) of NH2-uridine at several dihedral angles (Figure 5a−w) and the SAC-CI CD Boltzmann average spectrum (Figure 5x) were compared with the experimental CD spectrum (black) above 200 nm. In the experimental CD spectrum,[30] the first band was strongly positive at 268 nm (4.63 eV). The second and third bands were weakly negative at 237 nm (5.23 eV) and 216 nm (5.74 eV). The peak positions of the experimental CD spectrum of NH2-uridine were very similar to that of uridine, but the intensities of all bands were slightly weaker for NH2-uridine.

The experimental CD spectrum was in good agreement with the SAC-CI CD spectrum of the most stable anti-conformation (Figure 5k), as observed for uridine. However, the dihedral angle φ was different by about 2.8°. This difference is directly related to the difference of intensity between uridine and NH2-uridine. Both the shape and intensity of the SAC-CI CD spectrum with φ = 170° (Figure 5j) were very similar to that of uridine with φ = 173.9° (Figure 4j). Therefore, the difference between the experimental CD spectra of uridine and NH2-uridine reflects the difference of the optimized geometry based on the potential energy curve (Figure 3).

The SAC-CI CD spectral change for NH2-uridine with respect to the bond rotation was similar to that of uridine. When uridine rotates in the clockwise direction from the anti-conformation, the SAC-CI CD spectra with a broad positive peak were calculated from φ = 190° to φ = 270°. The peak with a negative sign appeared in the lowest energy region between φ = 290° and φ = 350° in the syn-region. The SAC-CI CD spectrum of the syn-conformer is completely opposite in sign as compared to the experimental CD spectrum (Figure 5t). The largest difference appeared between φ = 10° and φ = 30°. The features of the CD spectral change were very similar for both uridine and NH2-uridine. However, the intensity is weaker for NH2-uridine than for uridine between φ = 180° and φ = 230°. These differences contribute to the weak intensity of the experimental CD spectrum of NH2-uridine.

6. BOLTZMANN AVERAGED SAC-CI CD SPECTRA

Figure 3 indicates that the transformations between anti and syn may occur with low energy barriers for both uridine and NH2-uridine. In addition, the dihedral angle between uridine and ribose can change easily because both potential energy curves were flat in the anti-region. This implies that the observed spectra may reflect the statistical averaging over the rotations around these conformers. So, we calculated the existence ratios of each conformer. Tables 1 and 2 show the ratios of the existence of each conformer for uridine and NH2-uridine, assuming the Boltzmann distribution at 298.15 K, using the ground state Hartree−Fock/D95(d) energies. For uridine, more than 96% exists near the anti-region and less than 4% exists near the syn-region. However, for NH2-uridine, more than 99% exists near the anti-region and less than 1% exists near the syn region because the relative energy difference between anti- and syn-conformers is larger for NH2-uridine than for uridine. The existence ratio is more than 1% between φ = 140° and φ = 200° for uridine and between φ = 150° and φ = 240° for NH2-uridine because the potential energy curve is flatter in the anti-region for NH2-uridine than for uridine. Therefore, many conformers contribute to the CD spectra for NH2-uridine, compared with uridine.

The Boltzmann averaged SAC-CI CD spectra were in good agreement with the experimental CD spectra for both uridine (Figure 2a or 4x) and NH2-uridine (Figure 2c or 5x), although the Boltzmann averaged SAC-CI CD spectra were slightly different from the SAC-CI CD spectrum of the anti-conformer due to the contribution from surrounding conformers.

The difference between the Boltzmann averaged SAC-CI and experimental CD spectra was small for the first band. However, for the second and third bands of both uridine derivatives, the intensities of the Boltzmann averaged SAC-CI CD spectra were weaker than those of the experimental CD spectra. Considering from the SAC-CI CD spectra, the existence ratios at φ = 160° and 170° must be higher. Namely, the dihedral angle φ of the most-stable anti-conformer would be smaller than the calculated values (173.9° for uridine and 176.7° for NH2-uridine).

7. SAC-CI UV SPECTRA OF URIDINE

Next we examined what happened for the UV spectra with the conformational change. In Supporting Information Figure S2,

dx.doi.org/10.1021/jp501906u | J. Phys. Chem. A 2014, 118, 2931−2941

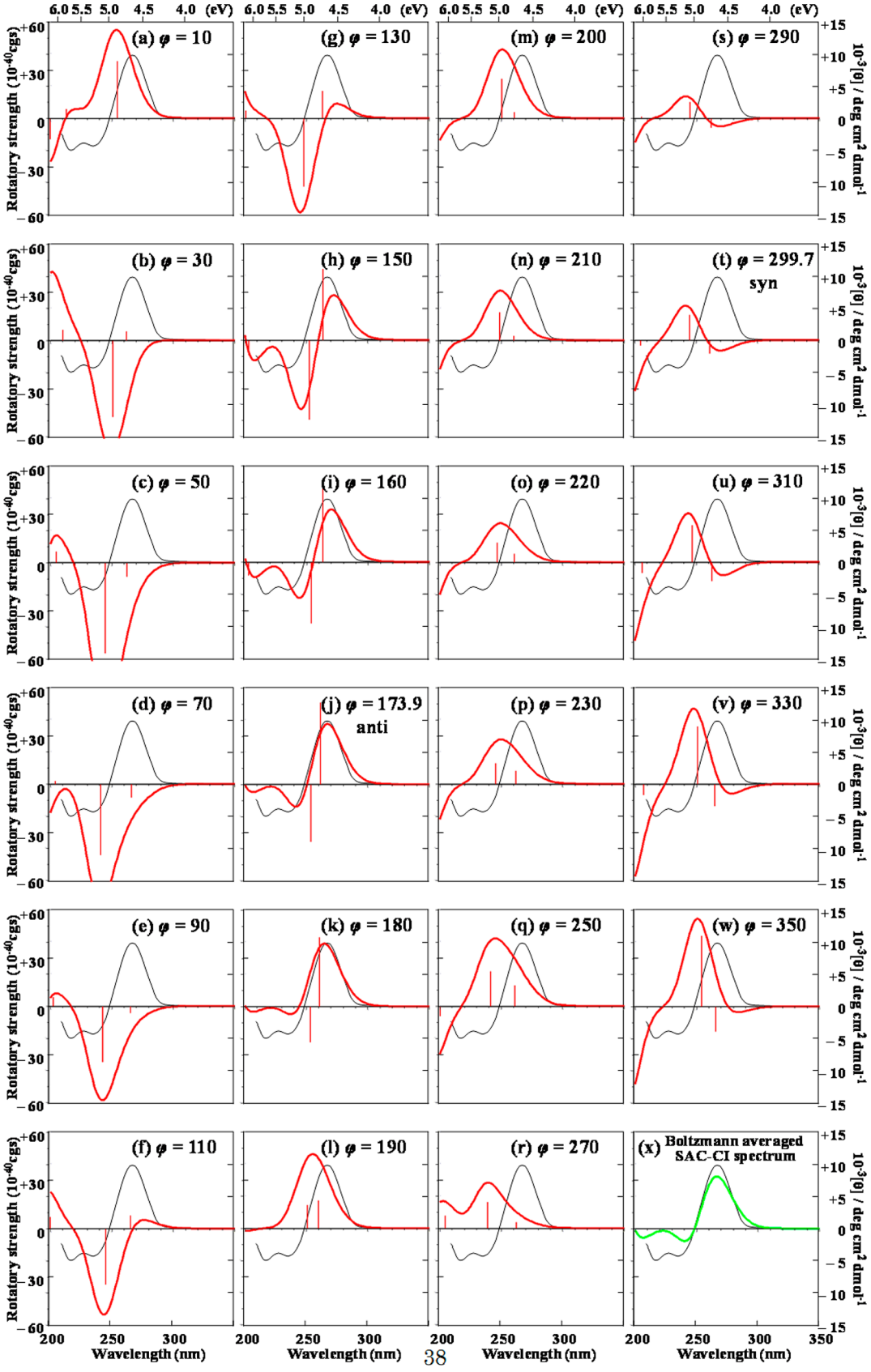

Figure 4. Experimental CD spectrum (black lines)[30] of uridine compared with the SAC-CI CD spectra (red lines) at several conformation angles φ (a–w) and the SAC-CI CD Boltzmann average spectrum (green line) (x).

the SAC-CI UV spectra of uridine at several dihedral angles were compared with the experimental UV spectrum (black) above 200 nm. Two bands were observed above 200 nm in the experimental UV spectrum. The lowest band was at 260 nm (4.77 eV)

dx.doi.org/10.1021/jp501906u | J. Phys. Chem. A 2014, 118, 2931–2941

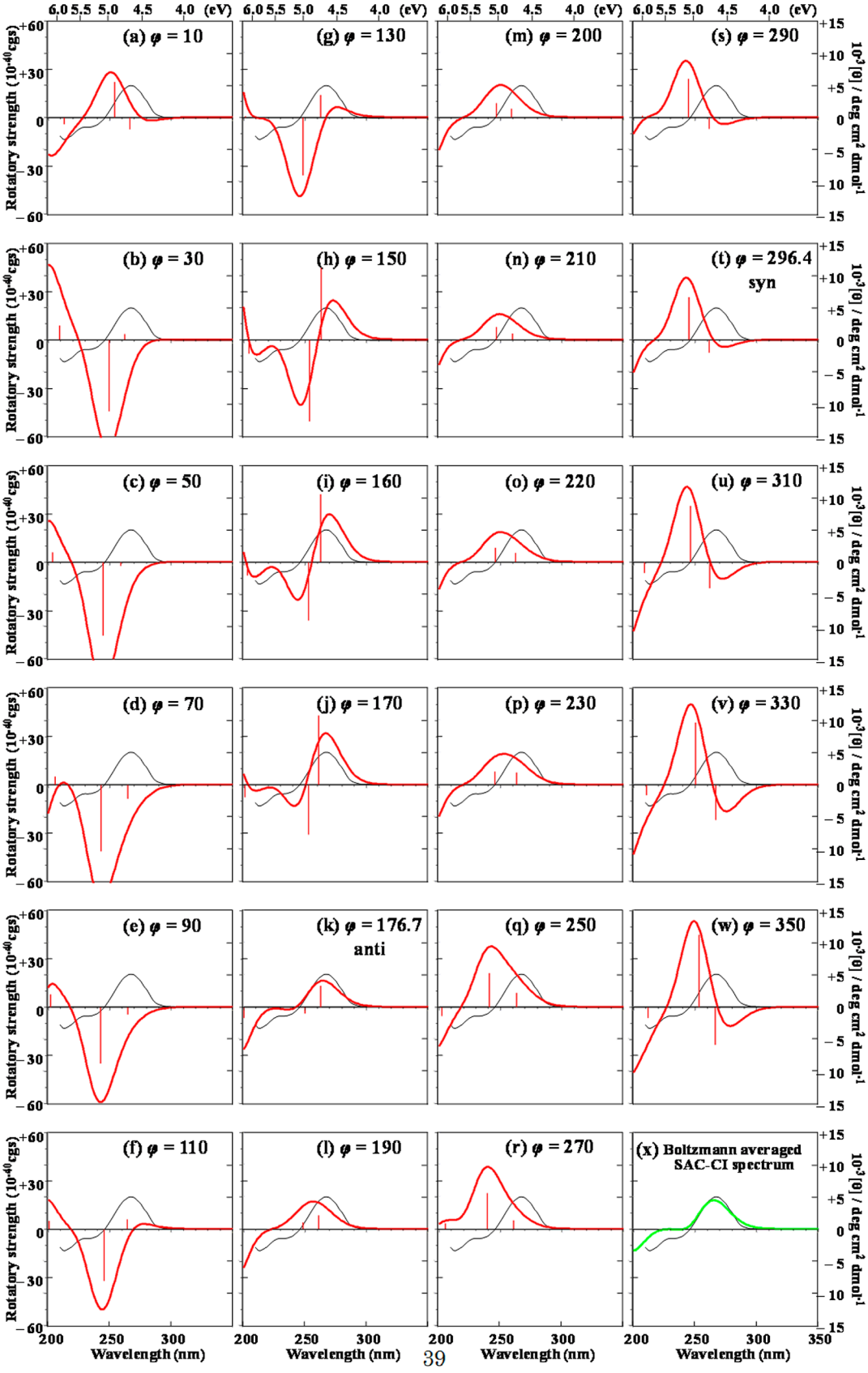

Figure 5. Experimental CD spectrum (black lines)[30] of NH2-uridine compared with the SAC-CI CD spectra (red lines) at several conformation angles φ (a–w) and the SAC-CI CD Boltzmann average spectrum (green line) (x).

and the second band was at 205 nm (6.05 eV). The experimental UV spectrum was in good agreement with the SAC-CI UV spectrum of the anti-conformer (Figure S2j, Supporting Information) as well as φ = 10° (Figure S2a, Supporting Information). This outcome

dx.doi.org/10.1021/jp501906u | J. Phys. Chem. A 2014, 118, 2931–2941

Table 3. Excited States of the Anti-Conformer of Uridine

	SAC-CI					experimental			
	EE[a]			Rot[c]		UV[d]		CD[e]	
	(eV)	(nm)	Osc[b]	(10^{-40} cgs)	nature	(eV)	(nm)	(eV)	(nm)
1^1A	4.74	262	0.02	50.76	$n-\pi^*$			4.64	267
2^1A	4.89	254	0.23	−35.89	$\pi-\pi^*$	4.77	260	5.28	235
3^1A	6.20	200	0.06	−6.34	$\pi-\pi^*$			5.71	217
4^1A	6.31	196	0.10	0.85	$\pi-\pi^*$	6.05	205		
5^1A	6.52	190	0.03	10.46	$\pi-\pi^*$				
6^1A	7.14	174	0.01	15.44	$n-\pi^*$				
7^1A	7.25	171	0.06	3.41	$n-\pi^*$				
8^1A	7.56	164	0.48	−25.10	$\pi-\pi^*$				
9^1A	8.07	154	0.01	41.50	$n-\pi^*$				
10^1A	8.88	140	0.01	−10.03	$\pi-\sigma^*$				

[a]Excitation energy. [b]Oscillator strength. [c]Rotatory strength. [d]Ref 31. [e]Ref 30.

Table 4. Excited States of the Anti-Conformer of NH2-Uridine

	SAC-CI					experimental			
	EE[a]			Rot[c]		UV[d]		CD[e]	
	(eV)	(nm)	Osc[b]	(10^{-40} cgs)	nature	(eV)	(nm)	(eV)	(nm)
1^1A	4.72	263	0.00	13.19	$n-\pi^*$			4.63	268
2^1A	4.95	250	0.25	−4.09	$\pi-\pi^*$			5.23	237
3^1A	6.19	200	0.00	−7.08	$n-\pi^*$			5.74	216
4^1A	6.38	194	0.16	−7.34	$\pi-\pi^*$				
5^1A	6.51	190	0.02	−0.47	$\pi-\pi^*$				
6^1A	7.02	177	0.02	−8.27	$n-\pi^*$				
7^1A	7.12	174	0.00	−0.85	$n-\pi^*$				
8^1A	7.40	168	0.02	31.39	$n-\pi^*$				
9^1A	7.55	164	0.35	−10.48	$\pi-\pi^*$				
10^1A	7.93	156	0.19	−144.20	$\pi-\sigma^*$				

[a]Excitation energy. [b]Oscillator strength. [c]Rotatory strength. [d]We cannot find the experimental data. [e]Ref 30.

indicates that the UV spectrum alone cannot determine the conformation of uridine because of its low sensitivity on the conformational change. The Boltzmann averaging UV spectrum was also almost the same shape and intensity as those of the anti-conformer because the SAC-CI UV spectrum was very similar between φ = 140° and φ = 200°.

8. EXCITED STATES OF THE STABLE ANTI-CONFORMER

We explained the excited states of the anti-conformers of both uridine derivatives in this section. Tables 3 and 4 show the excitation energies, oscillator strengths, rotatory strengths, and the natures of the excited states for both uridine and NH2-uridine, as compared with the experimental values.[30,31] The natures of the excited states are due to the orbitals of the nucleic acid base.

For the UV spectrum of uridine, the first band at 260 nm (4.77 eV) was assigned to the 2^1A excited state (4.89 eV), which is the $\pi-\pi^*$ transition of HOMO to LUMO. The second band at 205 nm (6.05 eV) was assigned to the 3 and 4^1A excited states (6.20 and 6.31 eV). The main configurations of both excited states were the excitation from HOMO to next-LUMO.

For the CD spectrum of uridine, the first band at 267 nm (4.64 eV) was assigned to the 1^1A excited state with the $n-\pi^*$ nature calculated at 4.74 eV. The second band at 235 nm (5.28 eV) was assigned to the 2^1A excited state calculated at 4.89 eV. The third band at 217 nm (5.71 eV) was assigned to the 3^1A excited state calculated at 6.20 eV. The excitation energy was lower by 0.39 eV for the 2^1A excited state and higher by 0.49 eV for the 3^1A excited state than the experimental value. However, the SAC-CI CD spectrum was in good agreement with the experimental CD spectrum because the Gaussian fitting changes the peak positions of the CD spectra. In the energy region between the 1 and 2^1A excited states, the intensity of the CD spectrum becomes weak because their rotatory strengths cancel each other. Therefore, in the experimental CD spectrum, the peak of the first band was observed at a lower-energy (higher-wavelength) region than the 1^1A excited state. However, the opposite occurred for the second band. Since the same occurred between the 3 and 4^1A excited states, the peak of the third band was observed at a lower-energy region than the 3^1A excited state.

The excitation energies of NH2-uridine were very similar to those of uridine. For the UV spectrum, the oscillator strength of the 2^1A state, corresponding to the first band, was 0.25 au for NH2-uridine, which is close to the value of 0.23 au for uridine. The oscillator strength of the 4^1A state, assigned to the second band, was 0.16 au, which was the same as the sum of the 3 and 4^1A states

However, the rotatory strength of the 1 and 2^1A states was weaker for NH2-uridine than for uridine. This result corresponds to the fact that the intensity of the experimental CD spectrum of NH2-uridine is weaker than that for uridine.

9. DIFFERENCE OF THE CD SPECTRA BETWEEN URIDINE AND NH2-URIDINE

The rotatory strength (R_{0a}) of the CD spectra is expressed using the angle θ between the electric transition dipole moment

dx.doi.org/10.1021/jp501906u | J. Phys. Chem. A 2014, 118, 2931−2941

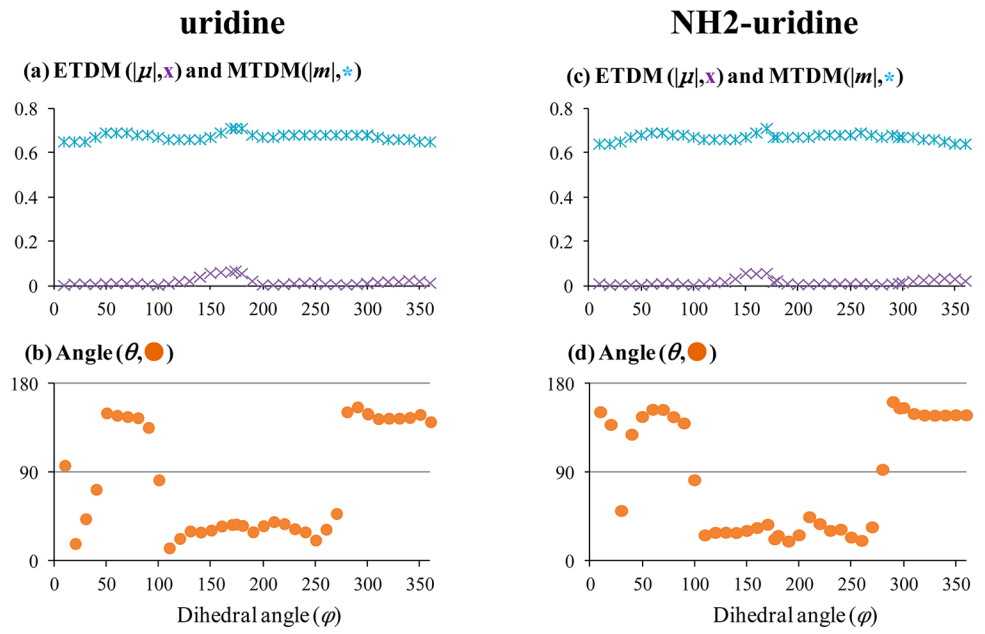

Figure 6. Electronic transition dipole moment (ETDM, $|\mu|$), the magnetic transition dipole moment (MTDM, $|m|$), and the angle (θ) of the first excited states of uridine and NH2-uridine.

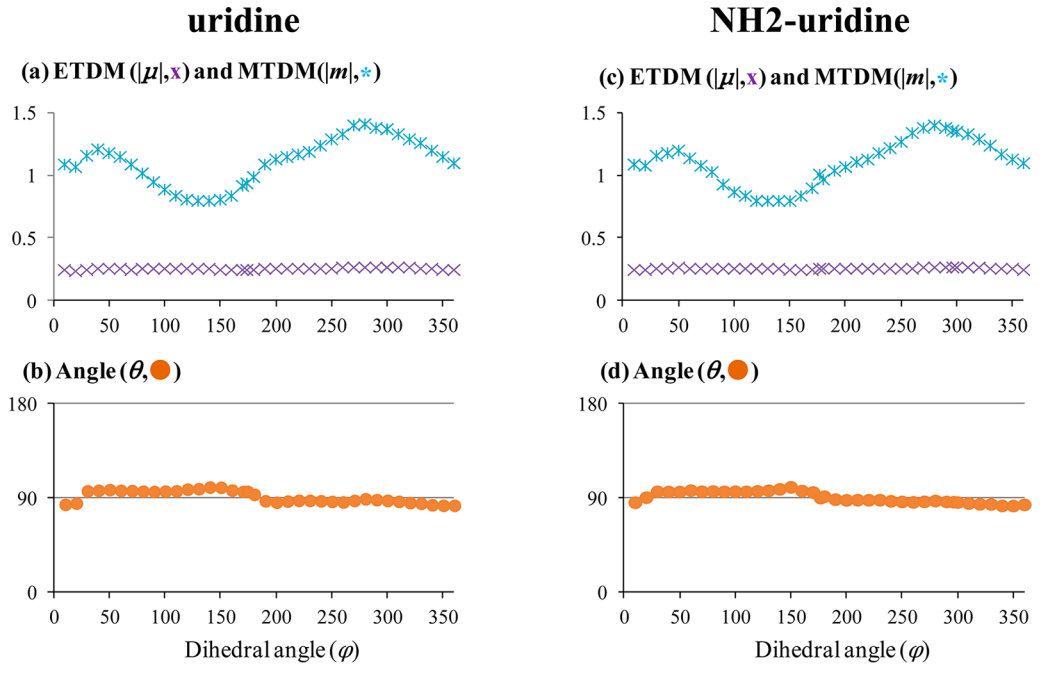

Figure 7. Electronic transition dipole moment (ETDM, $|\mu|$), the magnetic transition dipole moment (MTDM, $|m|$), and the angle (θ) of the second excited states of uridine and NH2-uridine.

(ETDM), $|\vec{\mu}_{0a}|$, and the magnetic transition dipole moment (MTDM), $|\vec{m}_{0a}|$, as

$$R_{0a} = \mathrm{Im}[|\vec{\mu}_{0a}||\vec{m}_{0a}|\cos\theta] \quad (2)$$

We extract the values (the transition dipole moments ($|\vec{\mu}_{0a}|$ and $|\vec{m}_{0a}|$) and the angle (θ)) from the SAC-CI results by the gauge-invariant equation (eq 1) and explain the difference of the CD spectra between uridine and NH2-uridine using eq 2. Figures 6 and 7 show the relationship between the three values (the transition dipole moments ($|\vec{\mu}_{0a}|$ and $|\vec{m}_{0a}|$) and the angle (θ)) and the dihedral angle (φ) for the 1 and 2^1A excited states, respectively, of both uridine derivatives. These data are shown in Supporting Information Tables S5−S12. In this section, we will clarify the difference between uridine and NH2-uridine using eq 2.

For the 1^1A excited state with the $n-\pi^*$ nature, the ETDM ($|\vec{\mu}_{0a}|$) is much weaker than the MTDM ($|\vec{m}_{0a}|$). Both ETDM and MTDM are independent of the dihedral angle (φ) and their magnitude are approximately constant. However, this state contains not only the $n-\pi^*$ nature but also the $\pi-\pi^*$ nature at the dihedral angles near the anti-conformer (between φ = 150 and 180° for uridine and between φ = 150 and 170° for NH2-uridine) (see Supporting Information Table S13). The mixing of the $\pi-\pi^*$ is reflected in the magnitude of the ETDM as shown in Figure 6a,c. Since the optimized dihedral angle (φ) was calculated

dx.doi.org/10.1021/jp501906u | J. Phys. Chem. A 2014, 118, 2931−2941

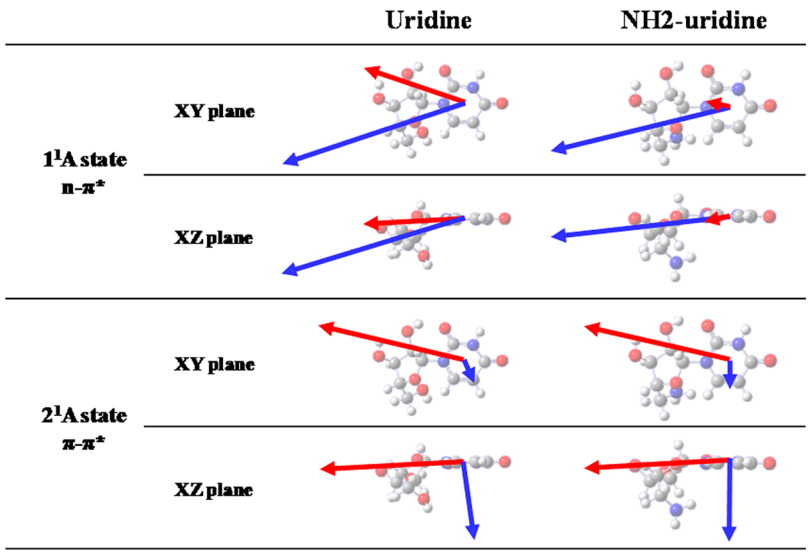

Figure 8. Direction of ETDM (red arrows) and MTDM (blue arrows) of the 1 and 2^1A excited states of the anti-conformers of uridine and NH2-uridine. The unit of arrows of the 2^1A state is 2.5 times larger than that of the 1^1A state. Uracil is on the *XY* plane.

to be 173.9° for uridine and 176.7° for NH2-uridine, the ETDM of the anti-conformer is strong for uridine (0.067) but weak for NH-uridine (0.016) (see Supporting Information Tables S5 and S9). This is the main reason for the fact that the intensity of the first band of NH2-uridine is weaker than that of uridine in the observed CD spectra.

In between the anti-conformer (φ = 176.7°) and φ = 190°, since the ETDM of NH2-uridine is weaker than that of uridine, the rotatory strength of the 1^1A excited state of NH2-uridine is weaker than that of uridine. The angle θ of NH2-uridine also differs from that of uridine by approximately 10 degrees. However, the contribution of the angle θ is small because of the function of cos θ.

The ETDM of the 1^1A state is very weak in comparison with the MTDM. Therefore, the direction of the ETDM is strongly affected by the position of ribose. Since the ETDM of the $n-\pi^*$ nature at φ = 100 and 280° is the weakest of all dihedral angles (Supporting Information Tables S5 and S9), the angle θ of the 1^1A state changes largely at φ = 100 and 280°. Therefore, the CD spectra vary largely at φ = 100 and 280°.

For the 2^1A excited states with $\pi-\pi^*$ nature, the moment $|\vec{\mu}_{0a}|$ is much stronger than that of the 1^1A excited state. The moment $|\vec{\mu}_{0a}|$ is approximately constant at all dihedral angles. However, the moment $|\vec{m}_{0a}|$ is weak between φ = 100 and 160° but strong between φ = 260 and 310° for both uridine derivatives (Figure 7a,c). Therefore, the moment $|\vec{m}_{0a}|$ is largely affected by the position of ribose in contrast to the moment $|\vec{\mu}_{0a}|$ for the 2^1A excited states. The angle θ is between 83 and 101° at all dihedral angles of both uridine derivatives. In the angle θ = 90°, the rotatory strength is equal to zero. The sign of the rotatory strength changes from negative to positive between φ = 180 and 190° for both uridine derivatives and from positive to negative around φ = 20° (see Supporting Information Table S6 and S10). The angle θ of the anti-conformer is calculated to be 96.7° for uridine but 90.7° for NH2-uridine. Therefore, the rotatory strength is strong for uridine but weak for NH2-uridine. This is the main reason that the intensity of the 2^1A excited state of NH2-uridine is weaker than that of uridine.

The values of two moments $|\vec{\mu}_{0a}|$ and $|\vec{m}_{0a}|$ and the angle θ are similar between uridine and NH2-uridine. Therefore, the relationship between the CD spectra and the dihedral angle is also similar between uridine and NH2-uridine. However, in the most-stable anti-conformer, there are slight difference in the values of $|\vec{\mu}_{0a}|$, $|\vec{m}_{0a}|$, and θ between uridine and NH2-uridine. For anti-conformers, the directions of ETDM and MTDM of the 1 and 2^1A excited states are shown in Figure 8. For the 1^1A excited state, the magnitude of the ETDM (red arrow) of NH2-uridine is weaker than that of uridine. For the 2^1A excited state, the angle θ of NH2-uridine is closer to 90° than uridine. Therefore, the contribution of each excited state of NH2-uridine to the rotatory strength is weaker than that of uridine. As a result, the observed CD spectrum of NH2-uridine is weaker than that of uridine.

10. CONCLUSIONS

The SAC-CI results shown here are truly ab initio: they are free from any frequency and intensity scaling, not like in the Td-DFT calculations. We have elucidated the differences between the CD spectra of uridine and NH2-uridine, although the models without solvent were used in this article. The intensity of the CD spectrum of NH2-uridine was weaker than that of uridine, although the excited states are very similar for the two molecules. The SAC-CI results showed that the CD spectra strongly depend on the dihedral angle between uracil and ribose. The SAC-CI CD spectrum of the syn-conformer is opposite in sign to that of the anti-conformer. Therefore, our theoretical results indicate that both uridine and NH2-uridine exist as the anti-conformer in solution. However, the dihedral angle of the most stable anti-conformation for uridine and NH2-uridine differs by 2.8°. This small variation in the dihedral angle changes the intensity and shape of the CD spectra. Their differences are due to the fact that the ETDM of NH2-uridine is weak for the first band and the fact that the angle θ of NH2-uridine is close to 90° for the second band.

However, in the UV spectra, the SAC-CI spectrum of uridine was in good agreement with the experimental spectrum. The differences between uridine and NH2-uridine were very small. Thus, it is difficult to analyze the conformation using the UV spectra alone, while the CD spectra are useful because of their very high sensitivity for the conformational changes.

The experimental CD and UV spectra of the uridine derivatives studied here are mainly of the intramolecular excitation nature within the nucleic acid bases. Therefore, the excited states

dx.doi.org/10.1021/jp501906u | J. Phys. Chem. A 2014, 118, 2931−2941

of NH2-uridine are almost the same as those of uridine. However, as noted in this article, the change of OH to NH2 caused a difference in the dihedral angle of the optimized geometry. The difference in the intensity of the CD spectra can be attributed to this structural change.

In the present study, we omitted the solvent. Therefore, the solvent may change the most stable conformation and the different stable conformation may strengthen the second and third bands of the SAC-CI CD spectra: the study of the solvent effect would be one of the most important subjects in the future.

In the ChiraSac study, we can elucidate the chemistry of chiral molecules and their interactions with the environmental molecules, using the reliable SAC-CI method as well as many other useful theoretical methods included in Gaussian09. By comparing the theoretical analysis with the experimental information, the ChiraSac provides the chemical information about the stable geometries of chiral molecules in solution or in confined environments such as in protein and in nanomaterials as well as the natures of the weak interactions such as the rotation around single bond, hydrogen-bonding or -stacking interactions, van der Waals force, solvent effect, etc. In the future, we expect that the ChiraSac will become the necessary and useful molecular technology for material and drug designs involving chirality.

■ ASSOCIATED CONTENT

Supporting Information

Atom labels (Figure S1), SAC-CI and experimental UV spectra of uridine (Figure S2), coordinates of the anti- and syn-conformers of uridine and NH2-uridine (Table S1−S4), the 1, 2, 3 and 4^1A excited states of uridine and NH2-uridine (Table S5−S12), and the coefficients of the HOMO−LUMO excitation of the 1^1A excited state of uridine and NH2-uridine (Table S13). This material is available free of charge via the Internet at http://pubs.acs.org.

■ AUTHOR INFORMATION

Corresponding Author

*(H.N.) E-mail: h.nakatsuji@qcri.or.jp. Phone: +81-75-634-3211. Fax: +81-75-634-3211.

Notes

The authors declare no competing financial interest.

■ ACKNOWLEDGMENTS

The computations were performed using the computers at the Research Center for Computational Science, Okazaki, Japan, whom we acknowledge. We also thank the support of Mr. Nobuo Kawakami for the researches of QCRI.

■ REFERENCES

(1) Berova, N., Nakanishi, K., Woody, R. W., Eds. *Circular Dichroism: Principles and Applications*; Wiley-VCH: New York, 2000.

(2) Miyahara, T.; Nakatsuji, H. Conformational Dependence of the Circular Dichroism Spectra of α-Hydroxyphenylacetic Acid: A ChiraSac Study. *J. Phys. Chem. A* **2013**, *117*, 14065−74.

(3) Nakatsuji, H.; Hirao, K. Cluster Expansion of the Wavefunction. Symmetry-Adapted-Cluster Expansion, Its Variational Determination, and Extension of Open-Shell Orbital Theory. *J. Chem. Phys.* **1978**, *68*, 2053−2065.

(4) Nakatsuji, H. Cluster Expansion of the Wavefunction. Excited States. *Chem. Phys. Lett.* **1978**, *59*, 362−364.

(5) Nakatsuji, H. Cluster Expansion of the Wavefunction. Electron Correlations in Ground and Excited States by SAC (Symmetry-Adapted-Cluster) and SAC-CI Theories. *Chem. Phys. Lett.* **1979**, *67*, 329−333.

(6) Nakatsuji, H. Cluster Expansion of the Wavefunction. Calculation of Electron Correlations in Ground and Excited States by SAC and SAC-CI Theories. *Chem. Phys. Lett.* **1979**, *67*, 334−342.

(7) Nakatsuji, H. Electronic Structures of Ground, Excited, Ionized, and Anion States Studied by the SAC/SAC-CI Theory. *ACH - Models Chem.* **1992**, *129*, 719−776.

(8) Nakatsuji, H. SAC-CI Method: Theoretical Aspects and Some Recent Topics. In *Computational Chemistry − Reviews of Current Trends*; Leszczynski, J., Ed; World Scientific: Singapore, 1997; Vol. 2, pp 62−124.

(9) Miyahara, T.; Hasegawa, J.; Nakatsuji, H. Circular Dichroism and Absorption Spectroscopy for Three-Membered Ring Compounds Using Symmetry-Adapted Cluster-Configuration Interaction (SAC-CI) Method. *Bull. Chem. Soc. Jpn.* **2009**, *82*, 1215−1226.

(10) Miyahara, T.; Nakatsuji, H.; Sugiyama, H. Helical Structure and Circular Dichroism Spectra of DNA: A Theoretical Study. *J. Phys. Chem. A* **2013**, *117*, 42−55.

(11) Niederalt, C.; Grimme, S.; Peyerimhoff, S. D.; Sobanski, A.; Vogtle, F.; Lutz, M.; Spek, A. L.; van Eis, M. J.; de Wolf, W. H.; Bickelhaupt, F. Chiroptical Properties of 12,15-Dichloro[3.0]-Orthometacyclophane: Correlations Between Molecular Structure and Circular Dichroism Spectra of a Biphenylophane. *Tetrahedron: Asymmetry* **1999**, *10*, 2153−2164.

(12) Vogtle, F.; Grimme, S.; Hormes, J.; Dotz, K. H.; Krause, N. Theoretical Simulations of Electronic Circular Dichroism Spectra. In *Interactions in Molecules Electronic and Steric Effects*; Peyerimhoff, S. D., Ed.; Wiley-VCH: Weinheim, Germany, 2003; pp 66−109.

(13) Jorge, F. E.; Autschbach, J.; Ziegler, T. On the Origin of Optical Activity in Tris-diamine Complexes of Co(III) and Rh(III): A Simple Model Based on Time-Dependent Density Function Theory. *J. Am. Chem. Soc.* **2005**, *127*, 975−985.

(14) Komori, H.; Inai, Y. Electronic CD Study of a Helical Peptide Incorporating *Z*-Dehydrophenylalanine Residues: Conformation Dependence of the Simulated CD Spectra. *J. Phys. Chem. A* **2006**, *110*, 9099−9107.

(15) Crawford, T. D.; Tam, M. C.; Abrams, M. L. The Current State of ab Initio Calculations of Optical Rotation and Electronic Circular Dichroism Spectra. *J. Phys. Chem. A* **2007**, *111*, 12057−12068.

(16) Botek, E.; Champagne, B. Circular Dichroism of Helical Structures Using Semiempirical Methods. *J. Chem. Phys.* **2007**, *127*, 204101−1−9.

(17) Giorgio, E.; Tanaka, K.; Verotta, L.; Nakanishi, K.; Berova, N.; Rosini, C. Determination of the Absolute Configurations of Flexible Molecules: Synthesis and Theoretical Simulation of Electronic Circular Dichroism/Optical Rotation of Some Pyrrolo[2,3-b]Indoline Alkaloids: A Case Study. *Chirality* **2007**, *19*, 434−445.

(18) Ding, Y.; Li, X. C.; Ferreira, D. Theoretical Calculation of Electronic Circular Dichroism of the Rotationally Restricted 3,8″-Biflavonoid Morelloflavone. *J. Org. Chem.* **2007**, *72*, 9010−9017.

(19) Bringmann, G.; Gulder, T. A. M.; Reichert, M.; Gulder, T. The Online Assignment of the Absolute Configuration of Natural Products: HPLC-CD in Combination with Quantum Chemical CD Calculations. *Chirality* **2008**, *20*, 628−642.

(20) Grkovic, T.; Ding, Y.; Li, X. C.; Webb, V. L.; Ferreira, D.; Copp, B. R. Enantiomeric Discorhabdin Alkaloids and Establishment of Their Absolute Configurations Using Theoretical Calculations of Electronic Circular Dichroism Spectra. *J. Org. Chem.* **2008**, *73*, 9133−9136.

(21) Shimizu, A.; Mori, T.; Inoue, Y.; Yamada, S. Combined Experimental and Quantum Chemical Investigation of Chiroptical Properties of Nicotinamide Derivatives with and without Intramolecular Cation−π Interactions. *J. Phys. Chem. A* **2009**, *113*, 8754−8764.

(22) Fan, J.; Ziegler, T. A Theoretical Study on the Exciton Circular Dichroism of Propeller-like Metal Complexes of Bipyridine and Tripodal Tris(2-pyridylmethyl)amine Derivatives. *Chirality* **2011**, *23*, 155−166.

(23) Lambert, J.; Compton, R. N.; Crawford, T. D. The Optical Activity of Carvone: A Theoretical and Experimental Investigation. *J. Chem. Phys.* **2012**, *136*, 114512−1−12.

(24) Bousquet, D.; Fukuda, R.; Maitarad, P.; Jacquemin, D.; Ciofini, I.; Adamo, C.; Ehara, M. Excited-State Geometries of Heteroaromatic Compounds: A Comparative TD-DFT and SAC-CI Study. *J. Chem. Theor. Comput.* **2013**, *9*, 2368−2379.
(25) Ehara, M.; Fukuda, R.; Adamo, C.; Ciofini, I. Chemically Iintuitive Indices for Charge-Transfer Excitation Based on SAC-CI and TD-DFT Calculations. *J. Comput. Chem.* **2013**, *34*, 2498−2501.
(26) Parr, R. G.; Yang, W. *Density-Functional Theory of Atoms and Molecules*; Oxford University Press: Oxford, U.K., 1989.
(27) Tomasi, J.; Mennucci, B.; Cammi, R. Quantum Mechanical Continuum Solvation Models. *Chem. Rev.* **2005**, *105*, 2999−3093.
(28) Cornell, W. D.; Cieplak, P.; Bayly, C. I.; Gould, I. R.; Merz, K. M., Jr.; Ferguson, D. M.; Spellmeyer, D. C.; Fox, T.; Caldwell, J. W.; Kollman, P. A. A Second Generation Force-Field for the Simulation of Proteins, Nucleic-Acids, and Organic-Molecules. *J. Am. Chem. Soc.* **1995**, *117*, 5179−5197.
(29) Frisch, M. J.; Trucks, G. W.; Schlegel, H. B.; Scuseria, G. E.; Robb, M. A.; Cheeseman, J. R.; Scalmani, G.; Barone, V.; Mennucci, B.; Petersson, G. A.; et al. *Gaussian 09*; Gaussian, Inc.: Wallingford, CT, 2009.
(30) Wada, T.; Minamimoto, N.; Inaki, Y.; Inoue, Y. Conformational and Orientational Switching of Uridine Derivatives by Borates. *Chem. Lett.* **1998**, *27*, 1025−1026.
(31) Miles, D. W.; Robins, R. K.; Eyring, H. Optical Rotatory Dispersion, Circular Dichroism, and Absorption Studies on Some Naturally Occurring Ribonucleosides and Related Derivatives. *Proc. Natl. Acad. Sci. U.S.A.* **1967**, *57*, 1138−1145.
(32) Dunning, T. H., Jr.; Hay, P. J. In *Methods of Electronic Structure Theory (Modern Theoretical Chemistry)*; Schaefer, H. F., III., Ed.; Plenum: New York, 1976; Vol. 3, pp 1−28.
(33) Nakatsuji, H. Cluster Expansion of the Wavefunction. Valence and Rydberg Excitations, Ionizations, and Inner-Valence Ionizations of CO_2 and N_2O Studied by the SAC and SAC-CI Theories. *Chem. Phys.* **1983**, *75*, 425−441.

■ NOTE ADDED AFTER ASAP PUBLICATION

This paper was published ASAP on April 11, 2014, with an error in the Supporting Information. The structures in Figure S1 were missing. The corrected Supporting Information was reposted on April 14, 2014.